PROCEEDINGS OF SPIE

SPIEDigitalLibrary.org/conference-proceedings-of-spie

A low-cost PVC-based dual-modality kidney phantom

Young, Jeff, Shahedi, Maysam, Dormer, James, Johnson, Brett, Gahan, Jeffrey, et al.

Jeff Young, Maysam Shahedi, James D. Dormer, Brett Johnson, Jeffrey Gahan, Baowei Fei, "A low-cost PVC-based dual-modality kidney phantom," Proc. SPIE 12034, Medical Imaging 2022: Image-Guided Procedures, Robotic Interventions, and Modeling, 120342Q (4 April 2022); doi: 10.1117/12.2611592

SPIE.

Event: SPIE Medical Imaging, 2022, San Diego, California, United States

Downloaded From: https://www.spiedigitallibrary.org/conference-proceedings-of-spie on 29 Apr 2022 Terms of Use: https://www.spiedigitallibrary.org/terms-of-use

A low-cost PVC-based dual-modality kidney phantom

Jeff Young [a], Maysam Shahedi [a,b], James D. Dormer [a,b],
Brett Johnson [c], Jeffrey Gahan [c], Baowei Fei [a,b,d,*]

[a] Department of Bioengineering, The University of Texas at Dallas, TX
[b] Center for Imaging and Surgical Innovation, The University of Texas at Dallas, TX
[c] Department of Urology, University of Texas Southwestern Medical Center, Dallas, TX
[d] Department of Radiology, University of Texas Southwestern Medical Center, Dallas, TX

* Email: bfei@utdallas.edu, Website: https://fei-lab.org

ABSTRACT

Phantoms are invaluable tools broadly used for research and training purposes designed to mimic tissues and structures in the body. In this paper, polyvinyl chloride (PVC)-plasticizer and silicone rubbers were explored as economical materials to reliably create long-lasting, realistic kidney phantoms with contrast under both ultrasound (US) and X-ray imaging. The radiodensity properties of varying formulations of soft PVC-based gels were characterized to allow adjustable image intensity and contrast. Using this data, a phantom creation workflow was established which can be easily adapted to match radiodensity values of other organs and soft tissues in the body. Internal kidney structures such as the medulla and ureter were created using a two-part molding process to allow greater phantom customization. The kidney phantoms were imaged under US and X-ray scanners to compare the contrast enhancement of a PVC-based medulla versus a silicone-based medulla. Silicone was found to have higher attenuation than plastic under X-ray imaging, but poor quality under US imaging. PVC was found to exhibit good contrast under X-ray imaging and excellent performance for US imaging. Finally, the durability and shelf life of our PVC-based phantoms were observed to be vastly superior to that of common agar-based phantoms. The work presented here allows extended periods of usage and storage for each kidney phantom while simultaneously preserving anatomical detail, contrast under dual-modality imaging, and low cost of materials.

Keywords: kidney phantom, mold casting, additive manufacturing, polyvinyl chloride (PVC), silicone, computed tomography (CT), ultrasound imaging, renal biopsy

1. INTRODUCTION

Percutaneous renal biopsy is an invasive medical procedure during which a needle is inserted into the kidney to extract a core tissue sample. Histologic examination of these tissue samples can yield valuable diagnostic information used to manage kidney diseases and tumors. Ultrasound (US) and X-ray computed tomography (CT) imaging are commonly used for both preoperative kidney lesion detection and localization and intraoperative guidance during a biopsy procedure. Of course, the most important factor in the minimization of complications during an image-guided percutaneous renal biopsy is operator proficiency[1]. Simulation training models that employed phantoms consisting of a porcine kidney inserted under a turkey breast showed improvements in successful retrieval of renal tissue, reduced procedure-related blood loss, and improved trainee confidence[2]. While porcine kidneys are able to mimic many renal biopsy conditions in human patients including kidney size, tissue echogenicity, and structural characteristics, consistency across different kidneys cannot be guaranteed and abnormal human anatomy cannot be reliably simulated. Likewise, biological materials are difficult to obtain, store, and work with. Previous work has demonstrated the production of a dual-modality agar and bovine gelatin-based kidney phantom for biopsy training, although major limitations included low durability and short shelf life at room temperature which required refrigeration to delay the growth of mold[3].

Recently, 3D printing technology has shown great promise for the development of realistic and sophisticated physical phantoms. Demand is increasing for phantoms that can accurately reflect various tissues and organs under multimodal imaging. However, direct printing of the phantom itself is limited by printer resolution and material compatibility with the 3D printer. Furthermore, many current 3D phantom printing approaches do not account for the time required, phantom durability, and cost of materials[4]. An indirect approach where a mold is 3D printed instead of the phantom itself can offer higher flexibility in material selection, allowing improved mimicry of tissue properties.

Medical Imaging 2022: Image-Guided Procedures, Robotic Interventions, and Modeling,
edited by Cristian A. Linte, Jeffrey H. Siewerdsen, Proc. of SPIE Vol. 12034, 120342Q
© 2022 SPIE · 1605-7422 · doi: 10.1117/12.2611592

Downloaded From: https://www.spiedigitallibrary.org/conference-proceedings-of-spie on 29 Apr 2022
Terms of Use: https://www.spiedigitallibrary.org/terms-of-use

In the past few years, there has been a great increase in the use of multimodality imaging. Various combinations of imaging modalities such as PET-CT and SPECT-CT integrate the anatomical structures with functional data, while combinations such as PET-MRI integrate multiple functional measurements. Biopolymer-based nanoparticles have been developed as CT and US dual-modal imaging contrast agents to enhance tumor diagnosis[5]. An augmented reality system integrated pre-operative CT data with the intra-operative US scans to provide real-time guidance in renal biopsy procedures[6]. Innovation in multimodality imaging can be aided with access to reliable and fast ways to test new imaging systems. Thus, a need is present for multimodal phantoms that better mimic tissue properties while retaining durability in between use, low material cost, and quick fabrication time.

In this study, our goal is to develop and evaluate a new approach for creating long-lasting, realistic kidney phantoms out of polyvinyl chloride (PVC)-plasticizer and silicone rubbers with contrast under both US and CT imaging.

2. METHODOLOGY

2.1 Materials

Two main types of materials were evaluated as components of the kidney phantom: soft PVC plastisol gels and silicone rubbers. The PVC-based phantom materials are inexpensive, commercially available products (regular hardness liquid plastic, plastic hardener, plastic softener, M-F Manufacturing Company, TX). These products consist of PVC and plasticizer in a solution form, which emulsify when heated to upwards of 350 °F and rapidly cure upon cooling to room temperature. While the exact chemical compositions are proprietary, many similar products are available from other sellers and are widely used to make soft lures and baits for fishing. Mold Star™ 30 (Smooth-On, Inc., Macungie, PA) was the second phantom material used in this study. It consisted of two platinum silicone rubbers that are mixed 1:1 by volume and cures after six hours. It has a low viscosity in its uncured state and a 30A Shore hardness after fully curing[7]. This material was chosen primarily for its flexibility, tear resistance, and negligible shrinkage. Cellulose powder (Sigmacell Type 20) and silica powder (MIN-U-SIL 40) were used as additional US contrast agents.

2.2 Methods and Data

A speed of sound study found that a PVC mixture with approximately 16% softener by volume showed an average speed of 1420.4 m/s and was determined to be a suitable material to mimic soft tissue (1540 m/s) for US imaging[8]. Based on this finding, we explored whether a mixture of regular plastic and softener or hardener could also mimic the Hounsfield unit (HU) values of kidney tissue. To characterize the radiodensities of varying combinations of the PVC solution with softener and hardener added, some multiple-well dishes were prepared containing the different soft plastic gels. As shown in Figure 1, each multiwell plate included combinations of regular liquid plastic with 20% hardener, 20% softener, 50% hardener, and 50% softener by volume, along with a cell of deionized water. An additional plate filled with uncured regular plastic, pure softener, and pure hardener was prepared for reference.

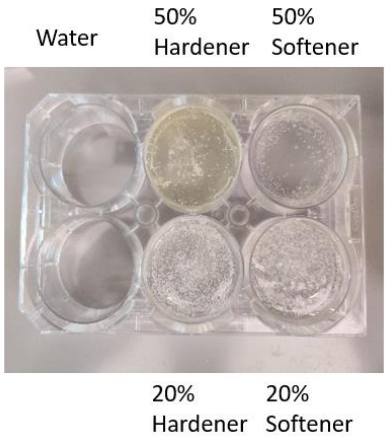

Figure 1. A multiwell plate containing PVC-based plastic gels with different formulas.

A 3D X-ray image of each plate was acquired using a Ziehm Vision RFD 3D C-arm (Ziehm Imaging Inc., Orlando, FL). Each image was exported as a series of DICOM files and visualized for analysis using the imshow3D MATLAB program[9].

Downloaded From: https://www.spiedigitallibrary.org/conference-proceedings-of-spie on 29 Apr 2022
Terms of Use: https://www.spiedigitallibrary.org/terms-of-use

A roughly cubic image patch for each plastic gel was selected from the 3D image volumes, and any extreme outlier voxels were excluded to lessen artifacts from air bubbles. Each selected region ranged in size from 20,000 to 50,000 voxels. The average of each region was then taken to give the approximate HU of a particular gel. This process was repeated five more times for each unique formulation of plastisol gel to give the average HU values. Silicone was prepared and imaged in a separate beaker.

2.3 Phantom Workflow

The first 3D printed kidney mold was based on the same manually segmented anonymized CT scan of a human patient that was used in a previous agar-based approach[3]. This first mold accurately displayed the kidney cortex and a partial ureter, but no internal complexity. We observed that the previous VeroClear material was not able to tolerate the 350 °F temperature that the plastisol needed to be heated to. The phantom mold began to exhibit cracks and warping around the edges after a few uses.

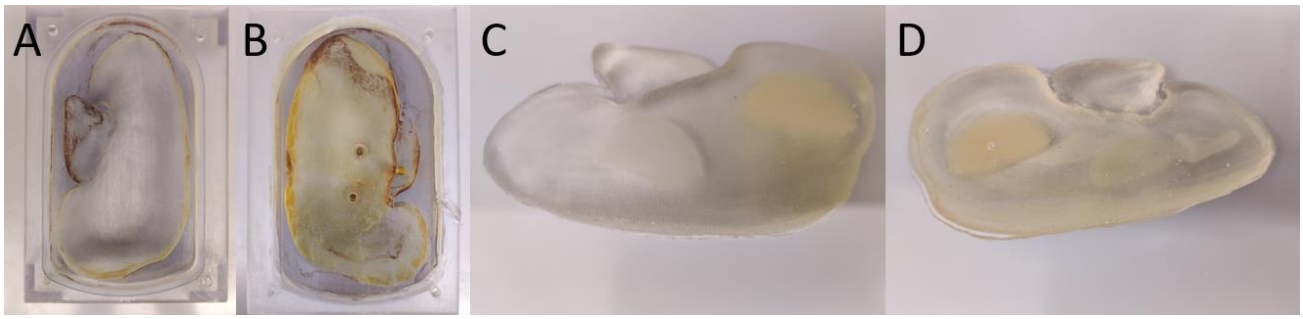

Figure 2. (A) 3D printed VeroClear kidney mold bottom, (B) VeroClear mold top, (C, D) Half kidney phantom with integrated lesions.

Initial tests sought to evaluate the visibility under CT/US imaging of different plastisol combinations with small amounts of contrast agents added. The phantom-making process started with the mixture of regular liquid plastic solution and softener/hardener in the ratios shown in Table 1. 0.15 g of cellulose powder was added to the mixture for lesion #1, and 0.15 g of silica powder was added to lesion #2. Each mixture was heated in a microwave under a fume hood in 20-second intervals until the temperature reached 350 °F measured by a thermocouple and the color became translucent. Simulated lesions were individually cast beforehand in a multiwell tray. Lesions with contrast agents are placed within the mold, and the liquid plastic is then poured in. Finally, the entire mold is partially submerged in an ice bath to accelerate cooling and shorten the curing time. The overall process from start to solid half kidney phantom was completed in less than two hours.

Table 1. List of material combinations that yield intended image contrast properties.

Lesion #1	Lesion #2	Kidney cortex
50% Regular Plastisol	50% Regular Plastisol	80% Regular Plastisol
50% Plastic Hardener	50% Plastic Hardener	20% Plastic Softener
0.15 g Cellulose (type 20)	0.15 g Silica powder (minusil 40)	

The final phantom creation workflow shown in Figure 3 aimed to achieve a more realistic internal structure to the complete kidney by including the anatomy of the medulla and part of the ureter. The kidney cortex mold was redesigned using Fusion360 (Autodesk Inc., San Rafael, CA) to have a 3 mm thicker edge on the top half, along with wider holes for injection points and gas escape. To prevent degradation of the mold over time, acrylonitrile butadiene styrene (ABS) was chosen as the new 3D printed mold material due to its higher melting point. Segmentations of the kidney medulla and ureter were combined and smoothed into a singular, continuous piece. This combined medulla and ureter were 3D printed with TangoPlus, a clear and flexible rubber-like material. The TangoPlus piece was placed inside the cortex mold, and hot plastisol with 20% softener was poured into the assembled mold. After cooling, the TangoPlus internal structure was removed, leaving a cavity in the cortex. The empty cortex was then placed back into the mold and filled with the plastisol-hardener mixture described in Table 2. Once the cavity was filled, a completed kidney phantom with soft plastic cortex

Downloaded From: https://www.spiedigitallibrary.org/conference-proceedings-of-spie on 29 Apr 2022
Terms of Use: https://www.spiedigitallibrary.org/terms-of-use

and hardened plastic medulla/ureter required less than 30 minutes of cooling. If both the cortex and internal structures were cast from plastic, submersion of the mold in an ice bath would result in a solid phantom in as little as 10 minutes. The TangoPlus piece was placed back into the cortex mold and the process was repeated with plastisol with 20% softener as the cortex and silicone as the filling, with a cure time of about six hours.

Our two-part molding process was enabled by the flexibility and tear resistance of both the plastisol cortex and the TangoPlus internal structure. By molding the internal structure of the kidney directly from a cavity left in the cortex, less 3D printing material is required than if an additional mold was used. This reduced both the total cost of the workflow and the time required for 3D printing. Additionally, a wider range of materials can be used to create the medulla and ureter because compatibility with a 3D printer is not required.

Table 2. List of ingredients for each component in the completed kidney phantoms.

Hard plastic medulla/ureter	Silicone medulla/ureter	Kidney cortex
50% Regular Plastisol 50% Plastic Hardener 0.2 g silica (Minusil 40) 0.1 g Calcium carbonate	Mold Star™ 30 Silicone	80% Regular Plastisol 20% Plastic Softener

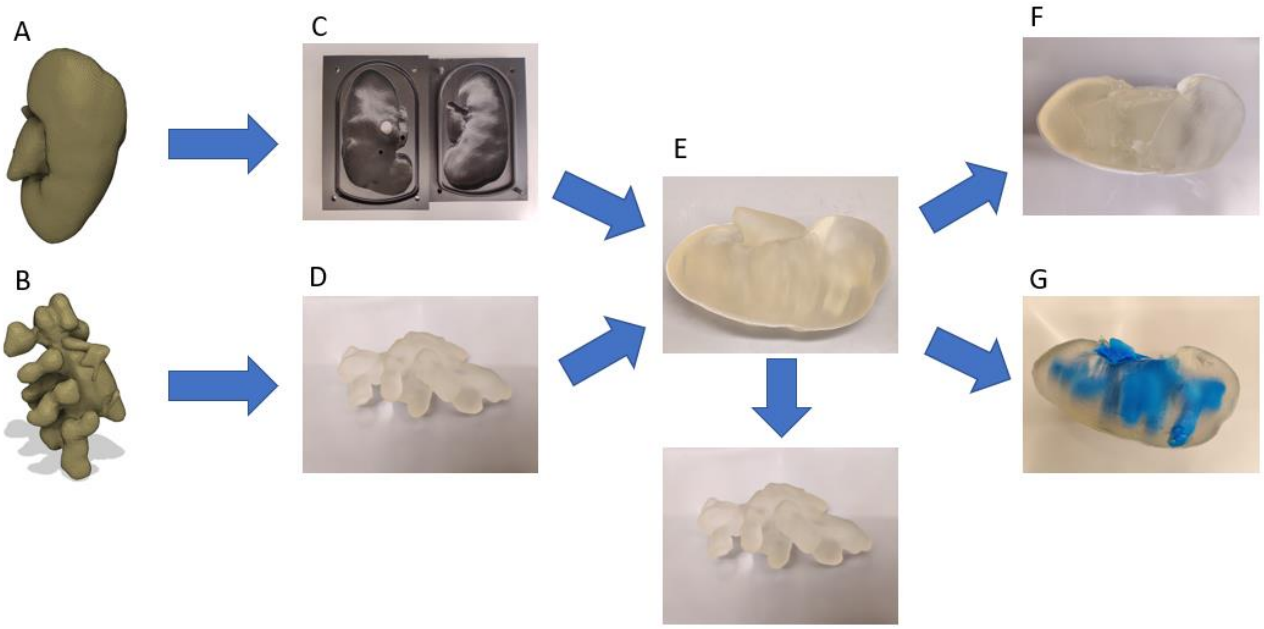

Figure 3. Phantom creation workflow: (A) Kidney cortex mesh, (B) kidney medulla and ureter mesh, (C) 3D printed ABS cortex mold, (D) 3D printed TangoPlus medulla and ureter, (E) plastic cortex around TangoPlus, (F) phantom with plastic medulla, (G) phantom with silicone medulla.

3. RESULTS

Figure 4 displays the HU distribution for each plastisol formulation in box plot format. The gels with 50% softener or 50% hardener displayed larger variations in HU than the gels with less softener or hardener added to them. While the HU could

Downloaded From: https://www.spiedigitallibrary.org/conference-proceedings-of-spie on 29 Apr 2022
Terms of Use: https://www.spiedigitallibrary.org/terms-of-use

vary between individual measurements, there was a clear trend of the HU being decreased by the addition of softener and increased by the addition of hardener. Table 3 lists the average HU for each material. Mold Star™ 30 Silicone had the largest HU value, comparable to soft tissue with iodinated contrast agents. Plastisol with 20% softener by volume was chosen to represent the kidney cortex, and plastisol with 50% hardener was chosen for the internal structures to maximize contrast.

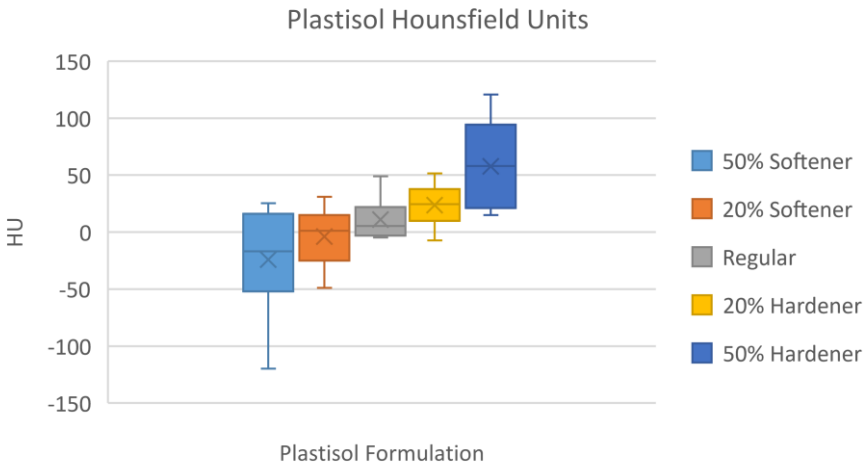

Figure 4. Hounsfield units were plotted for each unique formulation of plastisol.

Table 3. List of material combinations and their average Hounsfield unit values.

Material	Average HU
Plastic with 50% Softener	-24.188
Plastic with 20% Softener	-3.826
Regular Plastic	10.879
Plastic with 20% Hardener	23.608
Plastic with 50% Hardener	57.722
Mold Star™ 30 Silicone	302.66

The half kidney phantoms were imaged using the E14C4t triplane probe and 5P1 probe connected to a BK3000 system (BK Medical Holding Company, MA). Simulated lesions were easily visible under US imaging in Figure 5, showing clear contrast between lesion and cortex for both contrast agents. Visibility of lesions under CT imaging in Figure 6 required adjustment of the window and level but also demonstrated contrast enhancement. This demonstrated the viability of cellulose powder and silica powder to serve as contrast-enhancing agents in small quantities. No significant shrinkage of the phantoms was observed after storage at room temperature for more than six weeks, although slight color changes were present and the surface became oily to the touch after 12 weeks.

Downloaded From: https://www.spiedigitallibrary.org/conference-proceedings-of-spie on 29 Apr 2022
Terms of Use: https://www.spiedigitallibrary.org/terms-of-use

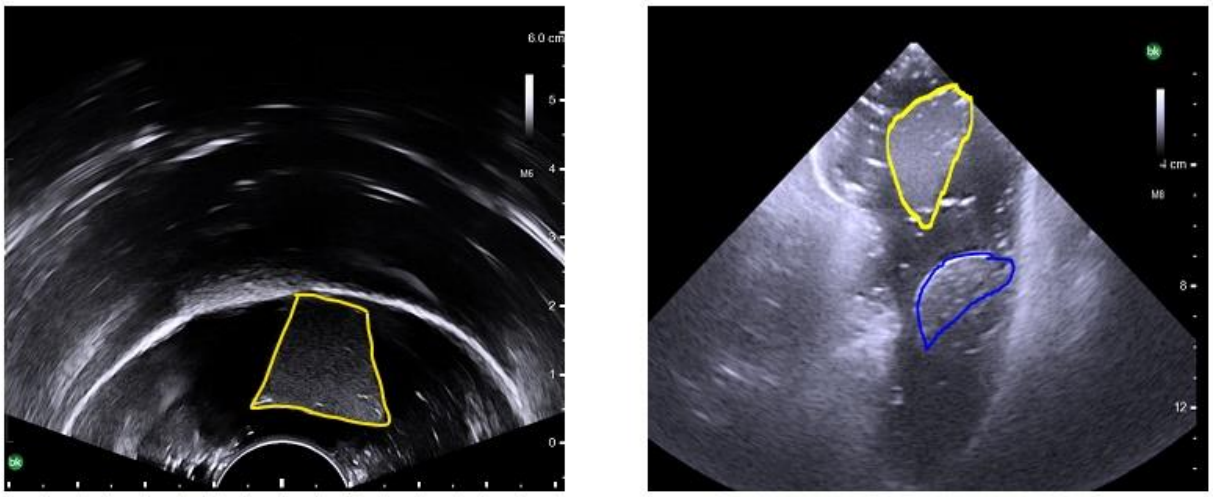

Figure 5. Ultrasound image of the half kidney phantom with lesion 1 visible (left). Ultrasound image of the half kidney phantom with both lesions visible (right).

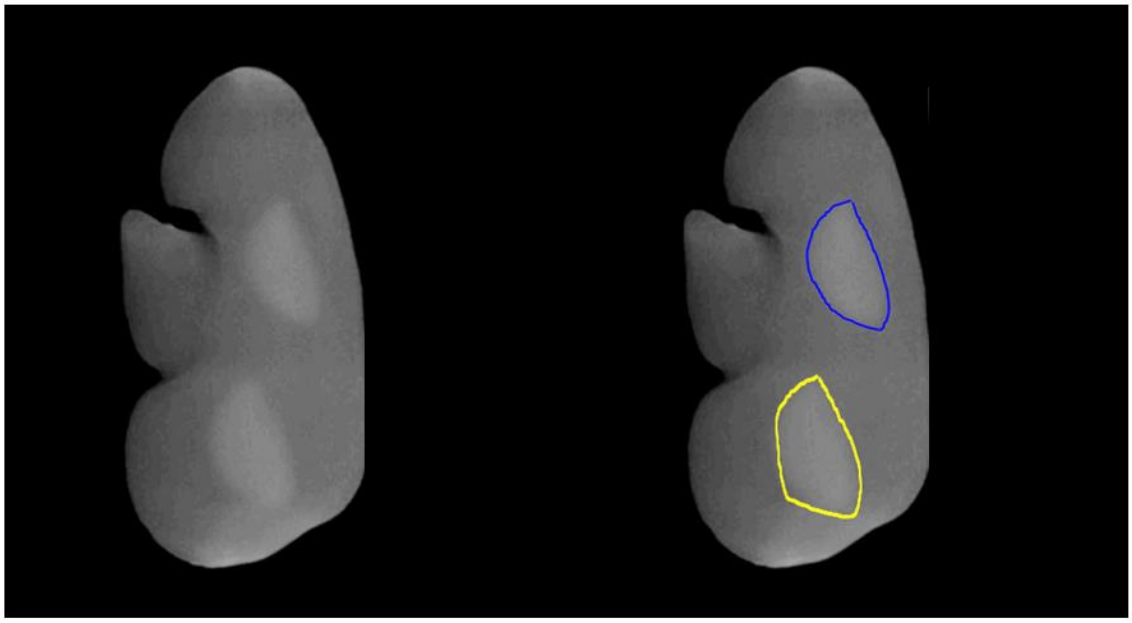

Figure 6. X-ray images of the half kidney phantom with both lesions visible (left). Lesion 1 is outlined in yellow and lesion 2 is outlined in blue (right).

Both plastic- and silicone-filled complete kidney phantoms were imaged with a 5P1 probe connected to a BK3000 US system and a Ziehm Vision RFD 3D C-arm. Figure 7 shows views of the plastic-filled kidney phantom under US imaging. There is a clear contrast between the cortex and the medulla, and the outer edge of the kidney cortex can mostly be delineated. Figure 7C shows the same cross-section of the phantom as Figure 7B, but with a compressing force applied to the midsection of the phantom. It can be observed that both the cortex and medulla deformed accordingly. The phantom returned to its original shape quickly after the force was removed, with no permanent effects.

Downloaded From: https://www.spiedigitallibrary.org/conference-proceedings-of-spie on 29 Apr 2022
Terms of Use: https://www.spiedigitallibrary.org/terms-of-use

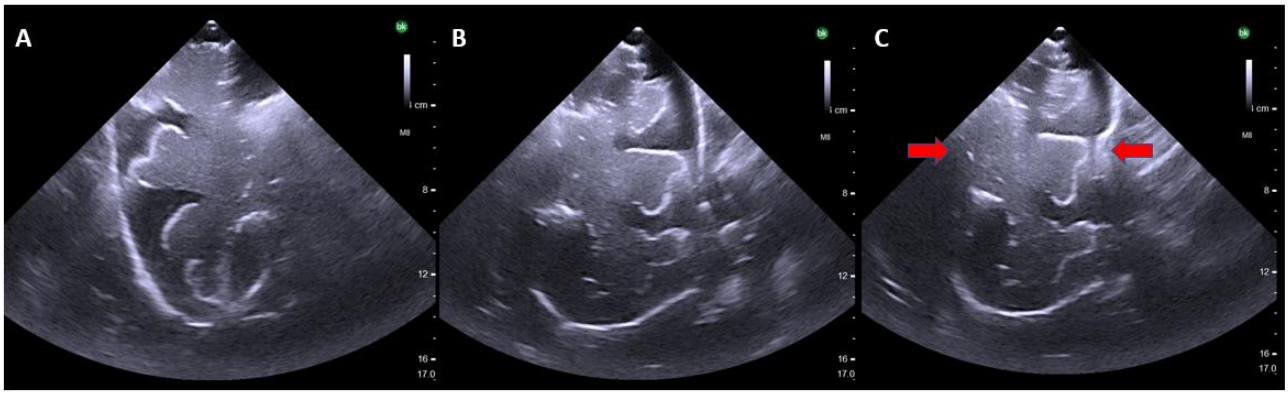

Figure 7. (A) Contrast enhancement of the internal structure was successful. (B) Alternate view of the phantom. (C) Red arrows indicate the location and direction of the applied force.

A plastisol-based internal structure of the medulla and part of the ureter was clearly distinguishable from the kidney cortex under CT imaging, as seen in Figure 8. Some air bubbles were observed in the phantom under both US and X-ray imaging, but visibility and contrast between the cortex and medulla were not impaired.

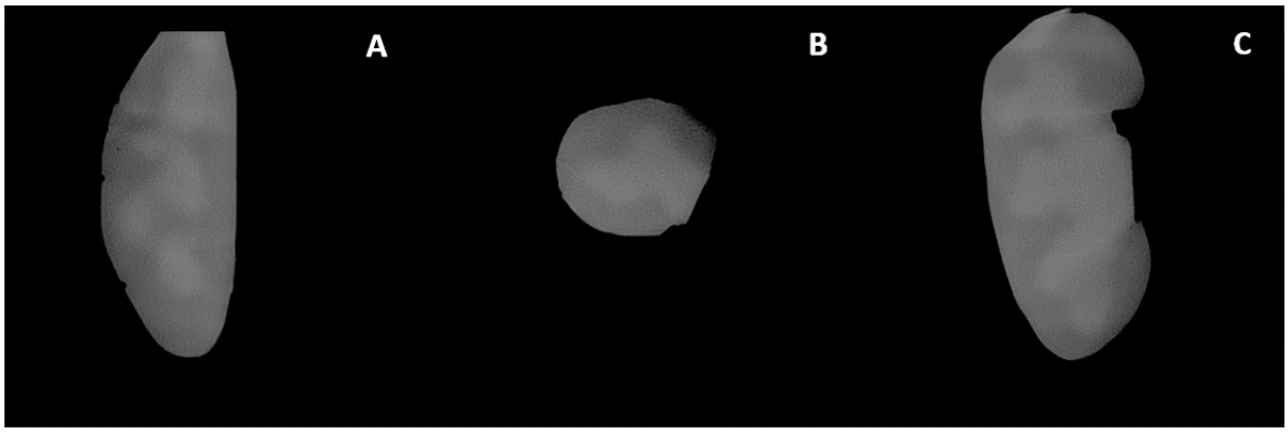

Figure 8. (A, B, C) Plastisol medulla phantom 3D CT slices parallel to sagittal, transverse, and coronal planes, respectively.

Upon completion of the silicone-filled kidney phantom, a thin layer of liquid uncured silicone surrounding the cured silicone was discovered. Even with assistance from a heat gun, this layer appeared to be permanently unable to fully cure. Some components of the plastisol cortex led to cure inhibition when in direct contact with the uncured silicone. Cure inhibition might be prevented by applying a layer of acrylic sealant prior to filling the plastic cortex cavity.

Silicone-based medulla had poor performance under US imaging compared to the PVC-plastisol medulla. As shown in Figure 9, the cortex edge was blurry and difficult to distinguish from the surroundings. In most of the angles and probe positions, the silicone appeared to attenuate the US waves to the point where no useful information could be obtained about structures behind the silicone. There were also some air bubbles visible under US imaging as small bright spots. Another reason for the poor quality of US signals could be an air gap between the medulla and cortex.

Downloaded From: https://www.spiedigitallibrary.org/conference-proceedings-of-spie on 29 Apr 2022
Terms of Use: https://www.spiedigitallibrary.org/terms-of-use

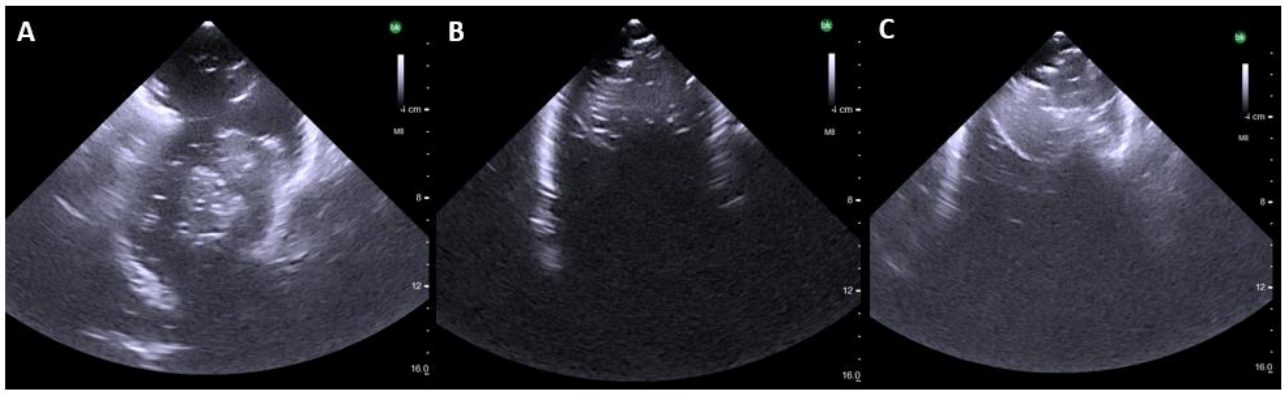

Figure 9. US images of phantom with silicone medulla/ureter. (A) Blurry outline of the cortex is visible, with some parts of the medulla visible, (B, C) Silicone medulla appears to overly attenuate US waves, resulting in poor visibility for the rest of the phantom.

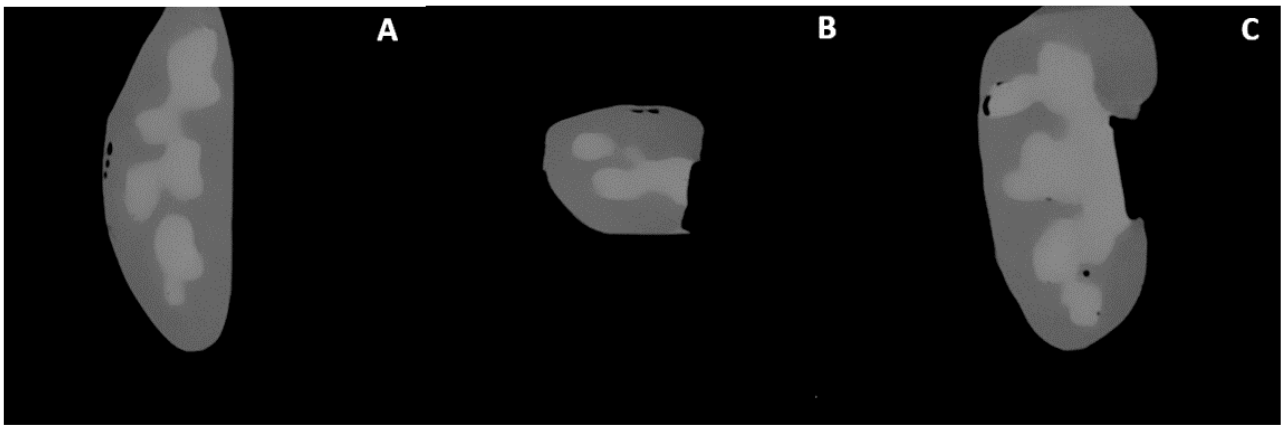

Figure 10. Silicone medulla phantom 3D X-ray slices parallel to sagittal (A), transverse (B), and coronal (C) planes.

Figure 10 displays the phantom with a soft plastic cortex and silicone medulla and ureter. Due to the large difference in HU values between the silicone and plastic, the contrast shown between the medulla and cortex was very strong. Air bubbles are visible as the dark spots inside the phantom.

4. DISCUSSION AND CONCLUSIONS

In this work, we demonstrated how a PVC-plastisol-based kidney phantom that contains the cortex, medulla, renal pelvis, and parts of the ureter could be created economically compared to commercial phantoms that can retail for upwards of $1000. Our characterization of the Hounsfield units of varying formulations of plastisol allows for simple adjustment of material compositions to match case-specific requirements. This information also enables future work to adopt a similar approach and mimic many other tissues in the body. Additionally, the long shelf life at room temperature and high durability allow for long-term storage and reuse of the same kidney phantom.

The plastisol gels introduced noticeable imaging artifacts on the 3D X-ray images. The artifacts could be because of the different 3D imaging and reconstruction of the 3D C-arm system. These artifacts, along with settling of the liquid plastisol during storage, likely account for the large HU variability observed in some gels. Acquiring additional images of our plastic gels with a full CT scanner would increase the precision of our data. A previous study that made use of PVC-plasticizer materials for abdominal phantom creation started with PVC in powder form which was measured by mass and manually mixed with plasticizer before heating[10]. Adopting this approach would prevent inconsistency due to settling in the liquid plastisol, and allow for greater fine-tuning of material properties. Physical properties of the PVC gels such as

Downloaded From: https://www.spiedigitallibrary.org/conference-proceedings-of-spie on 29 Apr 2022
Terms of Use: https://www.spiedigitallibrary.org/terms-of-use

Shore hardness and Young's modulus can be measured to optimally replicate soft tissue. Our two-step workflow would allow for the inclusion of complex internal structures, which enables more realistic organ deformation in abdominal phantoms developed to evaluate deformable registration algorithms.

One limitation of the phantom creation workflow was that the completed phantom only included a partial ureter and did not include any vascular structures. Improvements can be made in this area by redesigning the kidney cortex mold to accommodate a more extensive internal structure piece. It may be worthwhile to test different formulations of silicone elastomers for faster cure times and improved useability for US imaging. The ability to cleanly separate TangoPlus from the cured plastisol was a key contributor to the wider applicability of our workflow. In this manner, the thermoplastic properties of plastisol gel meant that the wait time until the phantom was ready for use only depended on how fast it could be cooled. Further work could utilize soft plastic phantoms to evaluate the performance of novel augmented/virtual reality surgical guidance systems when organs are subject to deformation.

ACKNOWLEDGMENTS

This research was supported in part by the U.S. National Institutes of Health (NIH) grants (R01CA156775, R01CA204254, R01HL140325, and R21CA231911), by the Cancer Prevention and Research Institute of Texas (CPRIT) grant RP190588.

REFERENCES

[1] Walker, P. D., Cavallo, T., and Bonsib, S. M., "Practice guidelines for the renal biopsy," Mod. Pathol. 17, 1555-1563 (2004).

[2] Dawoud, D., Lyndon, W., Mrug, S., Bissler, J. J., and Mrug, M., "Impact of ultrasound-guided kidney biopsy simulation on trainee confidence and biopsy outcomes," Am J Nephrol. 36(6), 570-574 (2012).

[3] Vargas, J., Le, P., Shahedi, M., Gahan, J., Johnson, B., Dormer, J. D., Shahub, S., Pfefferle, M., Judson, B. O., Alshara, Y., Li, Q., and Fei, B., "A complex dual-modality kidney phantom for renal biopsy studies," Proc. SPIE 11319, (2020).

[4] Filippou, V., and Tsoumpas, C., "Recent advances on the development of phantoms using 3D printing for imaging with CT, MRI, PET, SPECT, and ultrasound," Med. Phys. 45(9), 740-760 (2018).

[5] Choi, D., Jeon, S., You, D. G., Um, W., Kim, J.-Y., Yoon, H. Y., Chang, H., Kim, D.-E., Park, J. H., et al., "Iodinated echogenic glycol chitosan nanoparticles for X-ray CT/US dual imaging of tumor," Nanotheranostics 2(2), 117–127 (2018).

[6] Pfefferle, M., Shahub, S., Shahedi, M., Gahan, J., Johnson, B., Le, P., Vargas, J., Judson, B. O., Alshara, Y., et al., "Renal biopsy under augmented reality guidance," Medical Imaging 2020: Image-Guided Procedures, Robotic Interventions, and Modeling (2020).

[7] "Mold Star™ 30 product information.," Smooth-On, <https://www.smooth-on.com/products/mold-star-30/> (3 February 2022).

[8] Chiu, T., Xiong, Z., Parsons, D., Folkert, M. R., Medin, P. M., and Hrycushko, B., "Low-cost 3D print-based phantom fabrication to facilitate interstitial prostate brachytherapy training program," Brachytherapy 19(6), 800-811 (2020).

[9] Maysam, S., "imshow3D," MATLAB Central File Exchange, 29 October 2018, <https://www.mathworks.com/matlabcentral/fileexchange/41334-imshow3d> (15 August 2021).

[10] Liao, Y. L., Chen, H. B., Zhou, L. H., Zhen, X., "Construction of an anthropopathic abdominal phantom for accuracy validation of deformable image registration," Technology and Health Care 24(s2) (May 2016).

Downloaded From: https://www.spiedigitallibrary.org/conference-proceedings-of-spie on 29 Apr 2022
Terms of Use: https://www.spiedigitallibrary.org/terms-of-use